Received: 12 January 2024 | Accepted: 13 June 2024

DOI: 10.1097/HEP.0000000000001003

ORIGINAL ARTICLE

OPEN

Hepatic GDP-fucose transporter SLC35C1 attenuates cholestatic liver injury and inflammation by inducing CEACAM1 N153 fucosylation

Liangjun Zhang[1,2,3] | Pingfan Xie[1,2,3] | Mingqiao Li[1,2,3] | Xiaoxun Zhang[1,2,3] | Shuke Fei[4] | Nan Zhao[1,2,3] | Ling Li[1,2,3] | Qiaoling Xie[1,2,3] | Ziqian Xu[1,2,3] | Wan Tang[1,2,3] | Guanyu Zhu[1,2,3] | Zhixian Zhu[1,2,3] | Zuzhi Xu[5,6] | Jianwei Li[7] | Chengcheng Zhang[7] | James L. Boyer[8] | Wensheng Chen[1,2] | Shi-Ying Cai[8] | Qiong Pan[1,2,3] | Jin Chai[5,6]

[1]Department of Gastroenterology, the First Affiliated Hospital (Southwest Hospital), Third Military Medical University (Army Medical University), Chongqing, China

[2]Institute of Digestive Diseases of PLA, Southwest Hospital Third Military Medical University (Army Medical University), Chongqing, China

[3]Cholestatic Liver Diseases Center and Center for Metabolic-Associated Fatty Liver Disease, the First Affiliated Hospital (Southwest Hospital), Third Military Medical University (Army Medical University), Chongqing, China

[4]The Second Affiliated Hospital, Department of Hepatobiliary, Pancreatic and Splenic Surgery, Hengyang Medical School, University of South China, Hengyang, Hunan, China

[5]Department of Gastroenterology, Institute of Digestive Diseases of PLA, Cholestatic Liver Diseases Center and Center for Metabolic-Associated Fatty Liver Disease, the First Affiliated Hospital (Southwest Hospital), Third Military Medical University (Army Medical University), Chongqing, China

[6]The Second Affiliated Hospital, Hengyang Medical School, University of South China

[7]Institute of Hepatobiliary Surgery, Southwest Hospital, Third Military Medical University (Army Medical University), Chongqing, China

[8]Department of Internal Medicine and Liver Center, Yale University School of Medicine, New Haven, Connecticut, USA

Correspondence
Jin Chai, Department of Gastroenterology, Institute of Digestive Diseases of PLA, Cholestatic Liver Diseases Center and Center for Metabolic-Associated Fatty Liver Disease, the First Affiliated Hospital (Southwest Hospital), Third Military Medical University (Army Medical University), Chongqing 400038. The Second Affiliated Hospital, Hengyang Medical School, University of South China, Hunan 421001, China.
Email: jin.chai@cldcsw.org

Qiong Pan, Department of Gastroenterology, Third Military Medical University, Cholestatic Liver Diseases Center. The First Affiliated

Abstract

Background and Aims: Inflammatory response is crucial for bile acid (BA)-induced cholestatic liver injury, but molecular mechanisms remain to be elucidated. Solute Carrier Family 35 Member C1 (SLC35C1) can transport Guanosine diphosphate-fucose into the Golgi to facilitate protein glycosylation. Its mutation leads to the deficiency of leukocyte adhesion and enhances inflammation in humans. However, little is known about its role in liver diseases.

Approach and Results: Hepatic SLC35C1 mRNA transcripts and protein

Abbreviations: BA, bile acid; BDL, bile duct ligation; CA, cholic acid; CEACAM1, carcinoembryonic antigen-related cell adhesion molecule 1; ChIP, chromatin immunoprecipitation; CTR, control; DDC, diethoxycarbonyl-1, 4-dihydrocollidine; ER, endoplasmic reticulum; 2FF, 2-fluorofucose; GDP, guanosine diphosphate; iCCA, intrahepatic cholangiocarcinoma; LADII, leukocyte adhesion deficiency II; NPC, nonparenchymal cell; OC, obstructive cholestasis; PLC/PRF, Primary Liver Carcinoma/Poliomyelitis Research Foundation; SLC35C1, Solute Carrier Family 35 Member C1; TCA, taurocholic acid; WT, wild type.

Liangjun Zhang, Pingfan Xie, Mingqiao Li, Xiaoxun Zhang, and Shuke Fei contributed equally to this study and shared first authorship.

Supplemental Digital Content is available for this article. Direct URL citations are provided in the HTML and PDF versions of this article on the journal's website, www.hepjournal.com.

This is an open access article distributed under the terms of the Creative Commons Attribution-Non Commercial-No Derivatives License 4.0 (CCBY-NC-ND), where it is permissible to download and share the work provided it is properly cited. The work cannot be changed in any way or used commercially without permission from the journal.
Copyright © 2024 The Author(s). Published by Wolters Kluwer Health, Inc.

Hospital (Southwest Hospital), Third Military Medical University (Army Medical University), Chongqing 400038, China.
Email: qiong.pan@cldcsw.org

Shi-Ying Cai, Department of Internal Medicine, Yale University, New Haven 06510, USA.
Email: shi-ying.cai@yale.edu

Wensheng Chen, Department of Gastroenterology, Third Military Medical University Southwest Hospital, Chongqing 400038, China.
Email: wenshengchen@hotmail.com

expression were significantly increased in patients with obstructive cholestasis and mouse models of cholestasis. Immunofluorescence revealed that the upregulated SLC35C1 expression mainly occurred in hepatocytes. Liver-specific ablation of *Slc35c1* (*Slc35c1 cKO*) significantly aggravated liver injury in mouse models of cholestasis induced by bile duct ligation and 1% cholic acid–feeding, evidenced by increased liver necrosis, inflammation, fibrosis, and bile ductular proliferation. The *Slc35c1 cKO* increased hepatic chemokine Ccl2 and Cxcl2 expression and T cell, neutrophil, and F4/80 macrophage infiltration but did not affect the levels of serum and liver BA in mouse models of cholestasis. Liquid chromatography with tandem mass spectrometry analysis revealed that hepatic *Slc35c1* deficiency substantially reduced the fucosylation of cell-cell adhesion protein CEACAM1 at N153. Mechanistically, cholestatic levels of conjugated BAs stimulated SLC35C1 expression by activating the STAT3 signaling to facilitate CEACAM1 fucosylation at N153, and deficiency in the fucosylation of CEACAM1 at N135 enhanced the BA-stimulated CCL2 and CXCL2 mRNA expression in primary mouse hepatocytes and Primary Liver Carcinoma/Poliomyelitis Research Foundation/5-*ASBT* cells.

Conclusions: Elevated hepatic SLC35C1 expression attenuates cholestatic liver injury by enhancing CEACAM1 fucosylation to suppress CCL2 and CXCL2 expression and liver inflammation.

INTRODUCTION

The accumulation of bile acids (BAs) in the liver can induce cholestatic liver injury. When left untreated, this injury will progress to liver fibrosis, cirrhosis, and liver failure.[1,2] Our studies and those of others have shown that intrahepatic BAs can trigger an inflammatory response by stimulating the expression of chemokines (eg, CCL2 and CXCL2), which attract inflammatory immune cells (eg, neutrophils) that initiates hepatic cell injury.[3–5] Meanwhile, BAs can also trigger a negative feedback loop to repress excessive inflammation by activating the JAK/STAT3 and P38/MAPK signaling (eg, RUNX1 and IL32) and attenuate cholestatic liver injury.[6,7] However, it remains to be determined whether other mechanisms are involved in the pathology of BA-induced liver injury.

The Solute Carrier Family 35 Member C (SLC35C) genes, including *SLC35C1* and *SLC35C2*, encode nucleotide sugar transporters that transport Guanosine diphosphate-fucose from cytosol into the lumens of the Golgi apparatus and endoplasmic reticulum (ER) to facilitate protein glycosylation.[8–10] Both SLC35C1 and SLC35C2 are expressed in a broad range of organs and tissues, including the liver.[8,9] Specifically, SLC35C1 transports Guanosine diphosphate-fucose into the Golgi apparatus for protein N-fucosylation, whereas SLC35C2 is specifically required for protein O-fucosylation.[8,10,11] Mutations of SLC35C1 in humans can cause leukocyte adhesion deficiency II (LADII) and aggravate inflammation.[12–14] Upregulated expression of SLC35C1 is also observed in HCC and intrahepatic cholangiocarcinoma (iCCA),[15,16] but its functional role in liver diseases, especially in cholestasis, remains unclear.

Carcinoembryonic antigen-related cell adhesion molecule 1 (CEACAM1), also known as CD66a and biliary glycoprotein, is a highly glycosylated cellular adhesion molecule.[17] It is mainly expressed in epithelial cells (eg, hepatocytes), endothelial cells, and immune cells.[18] CEACAM1 can regulate cell differentiation, tumorigenesis and metastasis, insulin sensitivity, and mucosal immunity in various diseases, including HCC, NASH, and inflammatory bowel diseases.[19–23] In addition, *Ceacam1* deficiency exacerbates liver injury and inflammation through activating innate lymphoid and myeloid cells in a mouse model of autoimmune hepatitis.[20] Conversely, *Ceacam1* overexpression protects the liver from injury by reducing the diet-induced metabolic and inflammatory responses in liver-specific transgenic mice.[24] Together, these observations support the hypothesis that CEACAM1 functions as a negative repressor of the inflammatory response in the liver.[25,26] Interestingly, CEACAM1 is detected in the serum and bile of patients with obstructive jaundice, as

well as a rat model of cholestatic liver injury induced by bile duct ligation (BDL).[27,28] However, little is known on the role of hepatic CEACAM1 in cholestatic liver injury and the functional correlation between CEACAM1 and SLC35C1.

In this study, we investigated the expression and function of hepatic SLC35C1 in cholestasis. We found that hepatic SLC35C1 expression was significantly upregulated in patients with cholestasis and murine cholestatic models. Its deficiency in the mouse liver significantly aggravated cholestatic liver injury and inflammation, associated with decreased CEACAM1 N153 fucosylation, indicating that SLC35C1 was a negative regulator in cholestatic liver injury. These findings may help in developing novel therapeutic strategies for the treatment of cholestatic liver diseases.

METHODS

Reagents

Biotinylated aleuria aurantia lectin (B-1395-1) was purchased from Vector Laboratories (Newark, CA). Other special reagents including DMSO and various BAs, taurocholic acid (TCA), taurochenodeoxycholic acid, glycocholic acid, glycochenodeoxycholic acid, taurodeoxycholic acid, and cholic acid (CA), were from Sigma-Aldrich (St Louis, MO). APTSTAT3-9R (Cat# S8197), an inhibitor of STAT3 phosphorylation, was from Selleck Chem (Houston, TX). 2-Fluorofucose (2FF) (CAS# 2089647-47-0), a fucosylation inhibitor, was from MedChemExpress (Shanghai, China).

Patients with cholestasis

This study was carried out in accordance with the Declaration of Helsinki (2013) and the Declaration of Istanbul (2018) of the World Medical Association. The protocol for the human subject study was evaluated and approved by the Institutional Ethical Review Board at Southwest Hospital affiliated with Army Medical University (Chongqing, China). Individual human subjects signed a written informed consent before enrollment. Individual human subjects were enrolled in the Institute of Hepatobiliary Surgery and the Department of Gastroenterology at Southwest Hospital. Liver tissue samples were obtained at the time of surgery from 19 patients with obstructive cholestasis (OC), excluding primary biliary cholangitis, and 20 patients with noncholestasis metastatic liver cancer as the control (CTR) group. The diagnosis of these patients was further confirmed by liver histology and other laboratory examinations.[7] In addition, one patient with primary biliary cholangitis was diagnosed by liver biopsy specimens and was enrolled before any ursodeoxycholic acid treatment.[29] Clinical characteristics of these subjects were shown in Supplemental Tables S1, S2, http://links.lww.com/HEP/I541.

Animal experiments

All animal experiments were conducted in accordance with the guidelines of the Animal Care and Use Committee at Southwest Hospital (Chongqing, China) and approved by the Institutional Animal Care and Use Committee (Army Medical University).

Slc35c1$^{flox/flox}$ C57BL/6 J mice and *Alb*-Cre C57BL/6 J mice were generated by Shanghai Model Organisms Center (Shanghai, China). *Slc35c1*$^{flox/flox}$ mice were crossed with *Alb*$^{Cre/+}$ mice to generate *Slc35c1*$^{flox/flox}$/*Alb*$^{Cre/+}$ (*Slc35c1 cKO*) mice, which were genotyped by PCR of tail DNA using 2 pairs of primers. The sequences of primers were forward: 5′-GGCTGGCCTTGAATTT TATCCTG-3′ and reverse: 5′-GCACCACCCTCGGCT GAACT-3′ for *Slc35c1*; forward: 5′-TGGCAAACATACG CAAGGG-3′ and reverse: 5′- CGGCAAACGGACAGA AGCA-3′ for *Alb-Cre*. The first pair of primers were used to distinguish wild type (WT) (826 bp) from homozygous type (860 bp). The second pair of primers was used to detect the Cre gene (450 bp). Male 7-week-old C57BL/6J mice were purchased from the Center of Laboratory Animals of Southwest Hospital (Chongqing, China). The *Abcb4*$^{-/-}$ mice were generated as described.[6,30]

The 7-day BDL mouse model was described in a report.[7] Briefly, male WT mice were randomized to a sham operation (n = 4) or BDL (n = 5); male *Slc35c1*$^{flox/flox}$ and *Slc35c1 cKO* mice at 8 weeks old were subjected to a sham operation (n = 7 and 5, respectively) and BDL procedure (n = 5 for each genotype). For the 14-day 1% CA-fed mouse model, male WT mice were randomized into 2 groups and fed with 1% CA (n = 5) or rodent chow (n = 4); male *Slc35c1*$^{flox/flox}$ and *Slc35c1 cKO* mice were randomized and fed with rodent chow (n = 6 for each genotype) or 1% CA diet (n = 5 and 6, respectively). For the 3,5-diethoxycarbonyl-1, 4-dihydrocollidine (DDC) mouse model, male WT mice were randomized into 2 groups and fed with 0.1% DDC (n = 5) diet or rodent chow (n = 4) for 14 days. In the *Abcb4*$^{-/-}$ mouse model, WT and *Abcb4*$^{-/-}$ male mice at 8 weeks old were used (n = 6 for each genotype). All these experimental mice were housed and euthanized, as described.[7]

Primary hepatocyte isolation

Primary hepatocytes were isolated from 10- to 12-week-old *Slc35c1*$^{flox/flox}$ and *Slc35c1 cKO* mice and were maintained, as described.[31] Primary hepatocytes were treated with BAs for 12 or 24 hours. The relative levels of gene mRNA transcripts and protein expression were quantified by real-time quantitative PCR and western blot.[7]

Liquid chromatography with tandem mass spectrometry analysis

The N-linked glycans in mouse liver tissues (n = 5 for *Slc35c1*$^{flox/flox}$-BDL and *Slc35c1 cKO*-BDL, respectively) were analyzed using the Liquid chromatography with tandem mass spectrometry method by Shanghai Applied Protein Technology (China). The detailed procedures were described in the Supplemental Methods, http://links.lww.com/HEP/I541.

Cell culture and plasmid transfection

Human hepatoma Primary Liver Carcinoma/Poliomyelitis Research Foundation (PLC/PRF)/5-*ASBT* (apical sodium-dependent BA transporter overexpression) cells were maintained, as described.[31] Mouse *Ceacam1*-WT and *Ceacam1*-N153A mutant constructs were cloned into the pcDNA3.1 expression vector and tagged with FLAG. The DNA fragments for mouse *Slc35c1* and *Slc35c2* expression were also cloned into the pcDNA3.1 expression vector and tagged with histidine and MYC proto-oncogene tags, respectively. These constructs were obtained from Youbio Biological Technology (Xi' an, China). PLC/PRF/5-*ASBT* cells were treated with 2FF (100 μmol/L) for 2 days to determine protein fucosylation levels.

Luciferase reporter assays

The pcDNA3.1-*STAT3* plasmid for STAT3 overexpression (*STAT3 o/e*) was generated by Hunan Fenghui Biotechnology (Changsha, China). The pGL3-basic vectors containing human *SLC35C1* proximal promoter or its truncated forms (−1806, −898, −342, −272 to +36) were generated by PCR products with different primers in Supplemental Table S3, http://links.lww.com/HEP/I541. The pGL3-898/+36 was used to generate pGL3-*SLC35C1* 898MUT harboring mutations in a key motif of the potential STAT3 binding within the *SLC35C1* promoter region. These constructs were co-transfected with pGL3-*STAT3 o/e* or a CTR vector, together with the plasmid for the expression of Renilla luciferase gene, into PLC/PRF/5-*ASBT* cells. Twenty-four hours after transfection, the cells were treated with DMSO or 100 μM TCA for 12 hours. The luciferase activity in individual groups of cells was measured according to the protocol reported as described.[32]

Chromatin immunoprecipitation-PCR assay

Chromatin immunoprecipitation (ChIP) assays were performed using the Magna ChIP A/G Chromatin Immunoprecipitation Kit (Cat#17-10086; Millipore) according to the manufacturer's instructions.[31] Soluble chromatins were extracted from cultured PLC/PRF/5-*ASBT* cells or liver specimens of human subjects or mice. The chromatins were immunoprecipitated using STAT3-specific antibody (Supplemental Table S4, http://links.lww.com/HEP/I541). The resulting immunoprecipitants containing specific DNA were subjected to PCR amplification using specific primers. The sequences of primers and the sizes of the amplicons are listed in Supplemental Table S5, http://links.lww.com/HEP/I541.

Real-time quantitative PCR

Total RNA was extracted from different groups of cells or specimens and reverse transcribed into cDNA, as described[32] using the TaqMan probes and primers (Supplemental Table S6, http://links.lww.com/HEP/I541). The data were analyzed by $2^{-\Delta\Delta Ct}$.

Co-immunoprecipitation and western blot

Total proteins were extracted from individual liver tissue samples and different groups of cells, and the potential fucosylation in specific proteins was determined by co-immunoprecipitation using specific antibody and the rProtein A/G Magnetic IP/Co-IP Kit (ACE, #BK0004-02) by following the manufacturer's instructions. The precipitated proteins in magnetic beads were denatured in 2× SDS-PAGE protein loading buffer (BOSTER Biological Technology, AR0131-20) at 100 °C for 10 minutes. The proteins were resolved by SDS-PAGE in 10% gels and assayed by western blot, as described.[6,7] The pull-down assays with aleuria aurantia lectin to detect fucosylation levels of the protein. The specific antibodies are listed in Supplemental Table S4, http://links.lww.com/HEP/I541.

Liver histological analysis

Fresh mouse liver tissue samples were fixed in 10% formalin and paraffin embedded. The liver tissue sections (5 μm) were routine stained with hematoxylin and eosin and Sirius Red, as described.[6,7] The pathogenic degrees of liver histology were scored by expert pathologists in a blinded fashion.

Immunofluorescent and multiplex IF staining

The expression of SLC35C1, CK19, Na^+/K^+-ATPase, hepatic nuclear factor 4 alpha, CD8a, myeloperoxidase, and F4/80 for specific cell populations in liver tissues was examined by multiplex immunofluorescent, as

described.[31] CK19 and hepatic nuclear factor 4 alpha were used as specific markers for cholangiocytes or hepatocytes, respectively. Antibodies are shown in Supplemental Table S4, http://links.lww.com/HEP/I541.

Statistics

Data are expressed as the Mean ± SD of each group from at least 3 separate experiments. The difference between 2 groups was analyzed by an independent sample *t* test or Mann-Whitney *U* test, and comparison among groups was performed by one-way ANOVA or the Kruskal-Wallis test using GraphPad Prism 9.0. A *p*-value of < 0.05 was considered statistically significant.

RESULTS

Hepatic SLC35C1 expression is significantly upregulated in patients with cholestasis and mouse models of cholestasis

The relative levels of *SLC35C1* mRNA transcripts and protein expression in liver samples from patients with OC (n = 19) were 3.5- and 4.7-fold higher than samples from noncholestatic liver diseases controls (n = 20) (Figure 1A, B). Similarly, when compared with the healthy CTR mice, hepatic levels of *Slc35c1* mRNA transcripts in cholestatic mouse models were also significantly increased (Figure 1C), including 1% CA-fed mice, 0.1% DDC-fed mice, BDL mice, as well as *Abcb4*-KO mice. In contrast, there was no significant difference in the levels of hepatic *Slc35c2* mRNA expression between these cholestatic mouse models and their correspondent controls (Supplemental Figure S1A, http://links.lww.com/HEP/I541). Further multiplex immunofluorescent analysis revealed that SLC35C1 protein expression was higher in liver samples from patients with OC (Figure 1D), primary biliary cholangitis (Supplemental Figure S2A, http://links.lww.com/HEP/I541) as well as BDL mice (Supplemental Figure S2B, http://links.lww.com/HEP/I541) than that in their correspondent controls. Importantly, multiplex immunofluorescent also indicated that the upregulated SLC35C1 expression was predominantly detected in hepatocytes from both humans and mice when compared to other types of liver cells (Figure 1D and Supplemental Figure S2, http://links.lww.com/HEP/I541). Real-time quantitative PCR analysis of primary liver cells from adult mice revealed that the relative levels of *Slc35c1* mRNA transcripts were substantially higher in hepatocytes than in cholangiocytes and nonparenchymal cells (NPCs) (Supplemental Figure S3, http://links.lww.com/HEP/I541). These data were consistent with our preliminary observations of elevated SLC35C1 expression in cholestasis and indicated that upregulated SLC35C1 expression was mainly detected in hepatocytes.

Liver-specific ablation of Slc35c1 significantly aggravates cholestatic liver injury and inflammation without enhancing BA accumulation in the liver of mice

To investigate whether elevated SLC35C1 expression in cholestatic hepatocytes could contribute to the pathogenesis of liver injury, liver-specific knockout of *Slc35c1* (*Slc35c1 cKO*) mice was generated (Supplemental Figure S4, http://links.lww.com/HEP/I541) and subjected to BDL or 1% CA feeding. Liver function tests revealed that the levels of serum alanine aminotransferase, aspartate aminotransferase, and alkaline phosphatase were significantly higher in *Slc35c1 cKO*-BDL mice than that in the BDL-CTR mice (Supplemental Table S7, http://links.lww.com/HEP/I541). In contrast, there was no significant difference in the levels of serum total BAs (TBA) and liver tissue BAs between *Slc35c1 cKO*-BDL and BDL-CTR mice (Supplemental Table S7, http://links.lww.com/HEP/I541 and Figure 2C). Assessment of liver histology revealed that the degrees of liver necrosis and inflammation were significantly higher in *Slc35c1 cKO*-BDL mice than in BDL-CTR mice ($Slc35c1^{flox/flox}$), along with the increased scores of liver fibrosis and bile ductular proliferation (Figure 2A, B). Deficiency of liver-specific *Slc35c1* increased infiltrates of inflammatory Cd8a(+) T cell, myeloperoxidase(+) neutrophil, and F4/80(+) macrophage, as well as Ck19(+) bile ductular cells in the liver of mice after BDL (Figure 2A, D and Supplemental Figure S5, http://links.lww.com/HEP/I541). Aggravated liver injury was also detected in the 1% CA-fed *Slc35c1 cKO* mice (Supplemental Table S8, http://links.lww.com/HEP/I541). Of note, there was no significant difference in the levels of hepatic *Slc35c2* mRNA transcripts between *Slc35c1 cKO* mice and their controls, neither in 1% CA-fed or BDL models (Supplemental Figure S1C, D, http://links.lww.com/HEP/I541). Collectively, these data emphasized that hepatic *Slc35c1* deficiency exacerbated cholestatic liver injury and inflammation but did not significantly alter hepatic levels of BAs in mice.

Hepatic Slc35c1 deficiency markedly increases Ccl2 and Cxcl2 expression in cholestatic mouse livers and BA-treated primary mouse hepatocytes

To gain insights into the worsened liver injury and inflammation in the *Slc35c1 cKO*-BDL mice, the expression levels of genes involved in inflammation, fibrogenesis, and BA metabolism in the liver of mice were examined. There was no significant change in the relative levels of hepatic

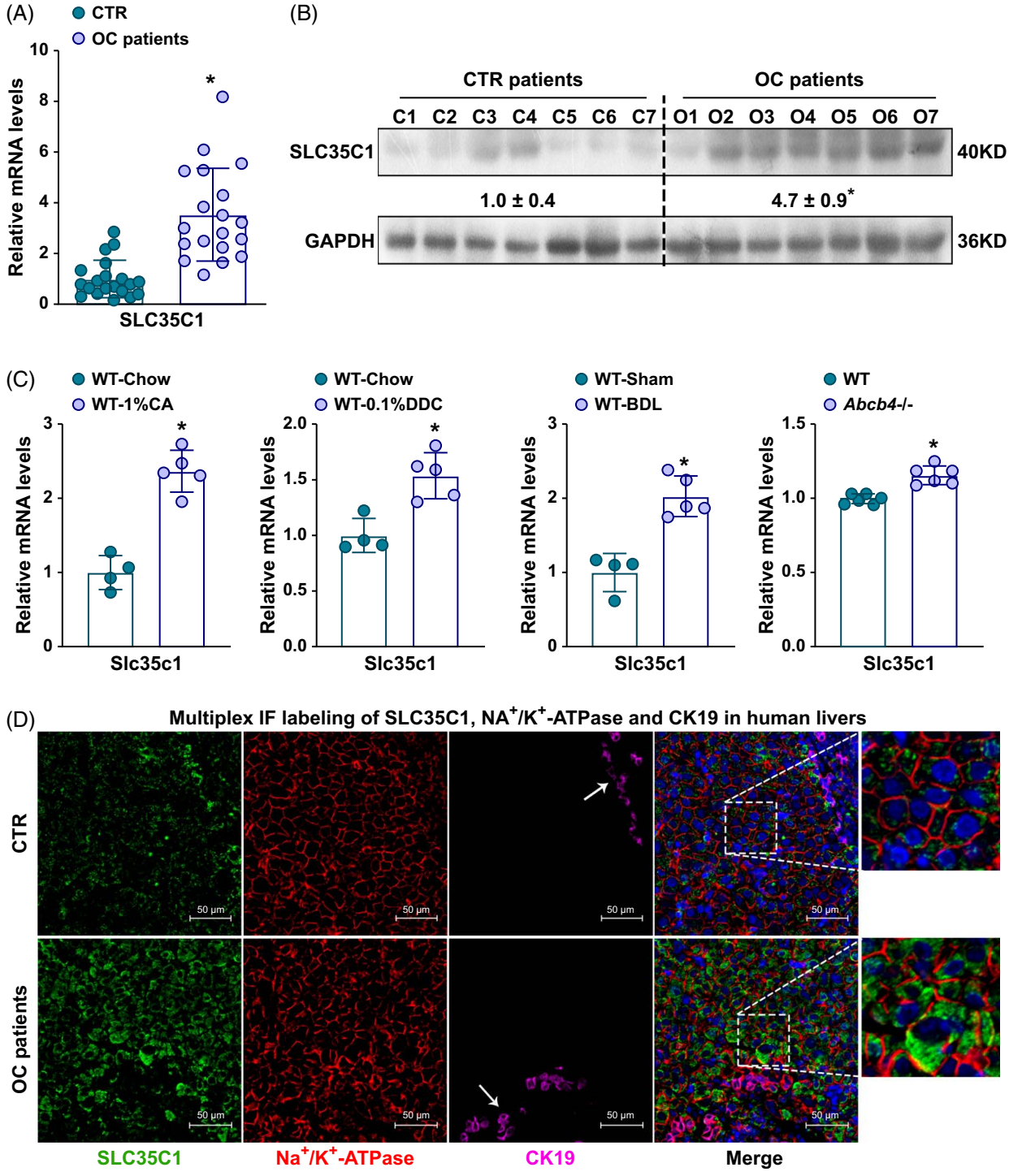

FIGURE 1 Upregulated hepatic SLC35C1 expression in patients and mice with cholestasis. The relative levels of SLC35C1 mRNA transcripts (A) and protein expression (B) in liver samples of patients with OC (n = 19) and patients with CTR (n = 20); O = OC, C = CTR. *$p < 0.05$ vs. the controls. (C) The relative levels of hepatic SLC35C1 mRNA transcripts in control mice (n = 4 or 6 for each model) and cholestatic mice, including 1% CA-fed, 0.1% DDC-fed, BDL, and *Abcb4* knockout mice (n = 5 or 6 for each model). *$p < 0.05$ vs. the control mice. (D) Multiplex immunofluorescent analysis of SLC35C1 (green color), Na^+/K^+-ATPase (red color, a specific marker for cell membranes), and CK19 (purple color, a specific marker for cholangiocytes) protein expression in a human OC liver and a control liver. White arrows, bile ducts. Abbreviations: BDL, bile duct ligation; CA, cholic acid; CTR, control; DDC, diethoxycarbonyl-1, 4-dihydrocollidine; GAPDH, glyceraldehyde-3-phosphate dehydrogenase; OC, obstructive cholestatic; SLC35C1, Solute Carrier Family 35 Member C1; WT, wild type.

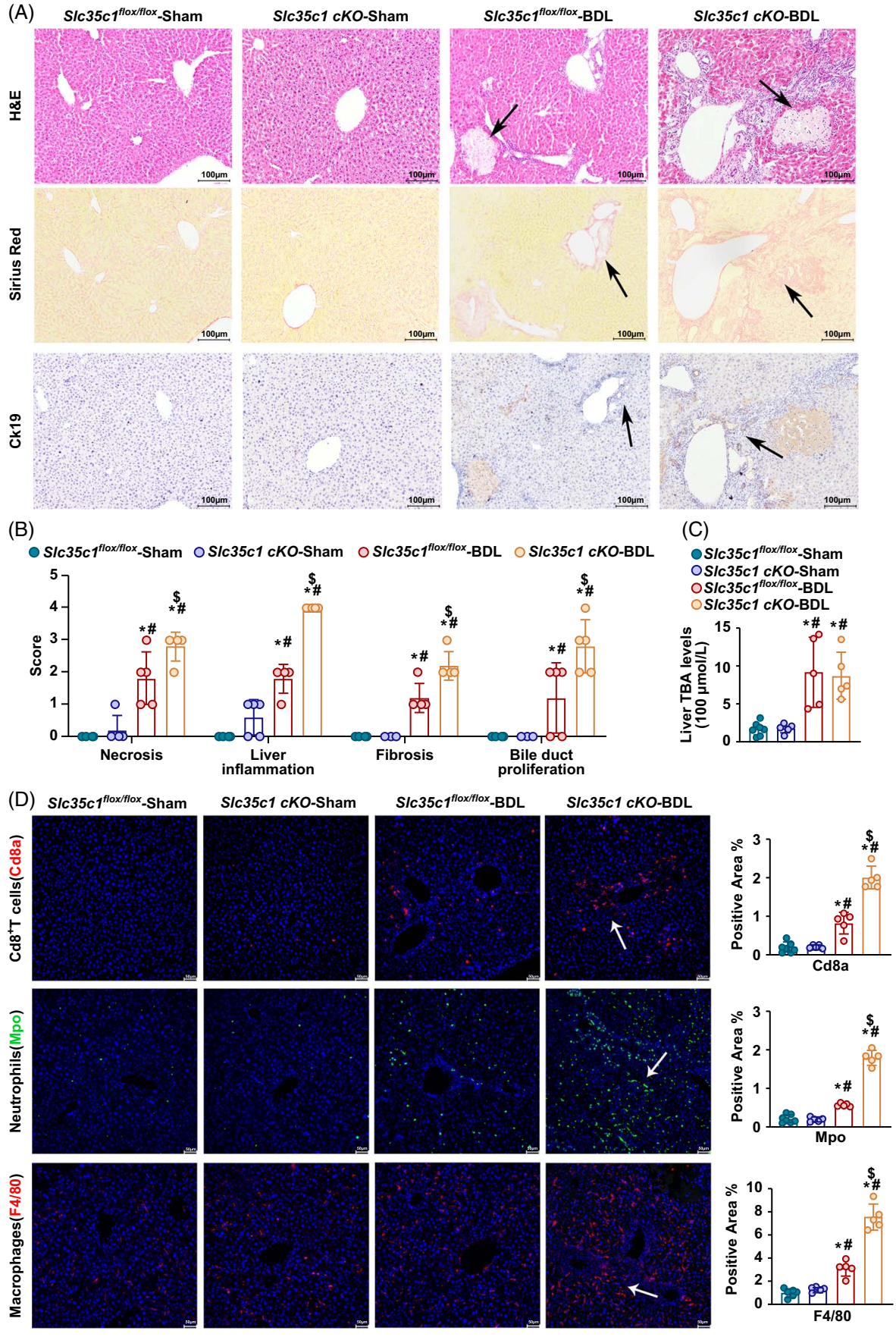
(A)
Slc35c1flox/flox-Sham
Slc35c1 cKO-Sham
Slc35c1flox/flox-BDL
Slc35c1 cKO-BDL
H&E
Sirius Red
Ck19
100μm
(B)
Slc35c1flox/flox-Sham
Slc35c1 cKO-Sham
Slc35c1flox/flox-BDL
Slc35c1 cKO-BDL
Score
Necrosis
Liver inflammation
Fibrosis
Bile duct proliferation
(C)
Slc35c1flox/flox-Sham
Slc35c1 cKO-Sham
Slc35c1flox/flox-BDL
Slc35c1 cKO-BDL
Liver TBA levels (100 μmol/L)
(D)
Slc35c1flox/flox-Sham
Slc35c1 cKO-Sham
Slc35c1flox/flox-BDL
Slc35c1 cKO-BDL
Cd8+T cells(Cd8a)
Neutrophils(Mpo)
Macrophages(F4/80)
Positive Area %
Cd8a
Mpo
F4/80

FIGURE 2 Liver-specific *Slc35c1* deficiency aggravates cholestatic liver injury and inflammation in BDL mice. (A) H&E staining, Sirius Red staining, and analysis of CK19 expression in the livers of control and *Slc35c1 cKO* mice following a Sham or BDL procedure. (B) The levels of inflammation, necrosis, fibrosis, and bile ductular proliferation were histologically assessed and scored by 2 expert pathologists in a blinded manner. N = 7 in the *Slc35c1*$^{flox/flox}$-sham group; N = 5 in the other 3 groups. (C) The levels of intrahepatic bile acids in control and *Slc35c1 cKO* mice following a sham or BDL procedure. (D) IF of Cd8a (red), Mpo (green), and F4/80 (red) expression, and nucleus (DAPI, blue) in the liver tissue sections. IF-positive areas were calculated using Image J (right). *$p < 0.05$ vs. the *Slc35c1*$^{flox/flox}$-sham mice; #$p < 0.05$ versus the *Slc35c1 cKO*-sham mice; $$p < 0.05$ vs. the *Slc35c1*$^{flox/flox}$-BDL mice. Abbreviations: BDL, bile duct ligation; H&E, hematoxylin and eosin; IHC, immunohistochemistry; Mpo, myeloperoxidase; SLC35C1, Solute Carrier Family 35 Member C1; TBA, total bile acid.

mRNA transcripts for the rate-limiting enzymes of BA synthesis (Cyp7a1 and Cyp8b1), metabolic enzymes (Cyp27a1, Cyp2b10, Cyp3a11, Cyp7b1, and Ugt1a1), and the key BA transporters (Bsep, Ntcp, Mrp2, Mrp4, Oatp3a1, and Ostβ) between *Slc35c1 cKO*-BDL group and BDL-CTR group (Figure 3A and Supplemental Figure S6A, http://links.lww.com/HEP/I541). Meanwhile, immunohistochemical staining with Ki67 in liver tissues, a marker of cell proliferation, did not show a significant difference between *Slc35c1 cKO*-BDL and BDL-CTR mice (Supplemental Figure S6B, http://links.lww.com/HEP/I541). In contrast, significantly higher levels of inflammatory cytokines, Tnfα and Il-6, chemokines, Ccl2 and Cxcl2, and their receptors, Ccr2 and Cxcr2 were detected in *Slc35c1 cKO*-BDL livers, when compared with that in the BDL-CTR livers (Figure 3B–D and Supplemental Figure S7A, B, http://links.lww.com/HEP/I541). We also detected higher levels of other inflammatory genes in the BDL livers, including Ccl4, Ccl7, Ccl20, Cxcl1, Cxcl15, Cxcl10, Cxcl11, Cxcl13, and Cxcl16, but the difference between *Slc35c1 cKO*-BDL livers and BDL-CTR livers did not reach statistical significance (Supplemental Figure S7C–K, http://links.lww.com/HEP/I541).

To examine whether the upregulated Ccl2 and Cxcl2 expression occurred in hepatocytes of cholestatic *Slc35c1 cKO* mice, primary hepatocytes were isolated from these animals and treated with TCA. As shown in Figure 3E and Supplemental Figure S8A, B, http://links.lww.com/HEP/I541, the relative levels of *Ccl2* and *Cxcl2* mRNA transcripts were significantly higher in the TCA-treated primary hepatocytes from *Slc35c1 cKO* mice than that in the TCA-treated primary hepatocytes from WT CTR mice. Conversely, *Slc35c1* overexpression blocked the TCA induction of *Ccl2* and *Cxcl2* mRNA expression in primary hepatocytes from WT mice (Figure 3E). Together, these data indicated that hepatic SLC35C1 inhibited the BA-induced Ccl2 and Cxcl2 expression in cholestastic hepatocytes.

Hepatic SLC35C1 induces the fucosylation of CEACAM1 at N153 to attenuate the BA-upregulated CCL2 and CXCL2 expression in hepatocytes during the process of cholestasis

SLC35C1 is a Guanosine diphosphate-fucose transporter that facilitates protein glycosylation. To investigate how SLC35C1 inhibited the BA-upregulated CCL2 and CXCL2 expression in hepatocytes, we performed glycoproteomic analyses in liver samples of *Slc35c1 cKO*-BDL and BDL-CTR mice. As demonstrated in Figure 4A, the levels of N-glycosylation in Ceacam1 (N153), Npc1 (N1063), and Sun1 (N834) proteins were significantly decreased in *Slc35c1 cKO*-BDL livers when compared with BDL-CTR livers, whereas the levels of N-glycosylation in Pld4 (N415), C4b (N1324), Clu (N327 and N353), Serpind1 (N167), Plod1 (N126), and Ubr5 (N2254 and N2255) were significantly increased. Because studies have shown that CEACAM1 functions as a repressor of inflammatory response in the liver,[25,26] and Ceacam1 was expressed in primary mouse hepatocytes (Supplemental Figure S9A, http://links.lww.com/HEP/I541), we assayed hepatic CEACAM1 expression in patients with OC and mouse models of cholestasis. We found that the relative levels of hepatic CEACAM1 mRNA transcripts and protein expression were significantly lower in patients with OC and cholestatic mice than in their respective controls (Supplemental Figure S9B, E, http://links.lww.com/HEP/I541). In contrast, the fucosylation of CEACAM1 was dramatically increased in liver tissues of patients with OC when compared with patients with CTR (Supplemental Figure S9F, http://links.lww.com/HEP/I541). Notably, genetic ablation of hepatic *Slc35c1* did not affect hepatic Ceacam1 mRNA and protein expression in mice (Supplemental Figure S9C, D, http://links.lww.com/HEP/I541). These data suggest that SLC35C1 may mediate CEACAM1 fucosylation at N153 to modulate liver inflammation in cholestasis.

To further examine this possibility, we constructed the plasmids for the expression of CEACAM1-WT and mutant (replacing Asparagine 153 with an Alanine, N153A) and transfected them into PLC/PRF/5-*ASBT* cells. Strikingly, WT CEACAM1 overexpression, but not the CEACAM1-N153A mutant, completely abolished the TCA-upregulated CCL2 and CXCL2 mRNA expression in PLC/PRF/5-*ASBT* cells (Figure 4B and Supplemental Figure S10A, http://links.lww.com/HEP/I541). Similar to the results with the CEACAM1-N153A mutation, treatment with 2FF, a fucosylation inhibitor,[33,34] also did not repress the TCA-upregulated CCL2 and CXCL2 mRNA expression in PLC/PRF/5-*ASBT* cells (Figure 4C). Studies have reported that hepatic EGR1 expression is upregulated in patients with OC and cholestatic mice; conjugated BAs also stimulate EGR1

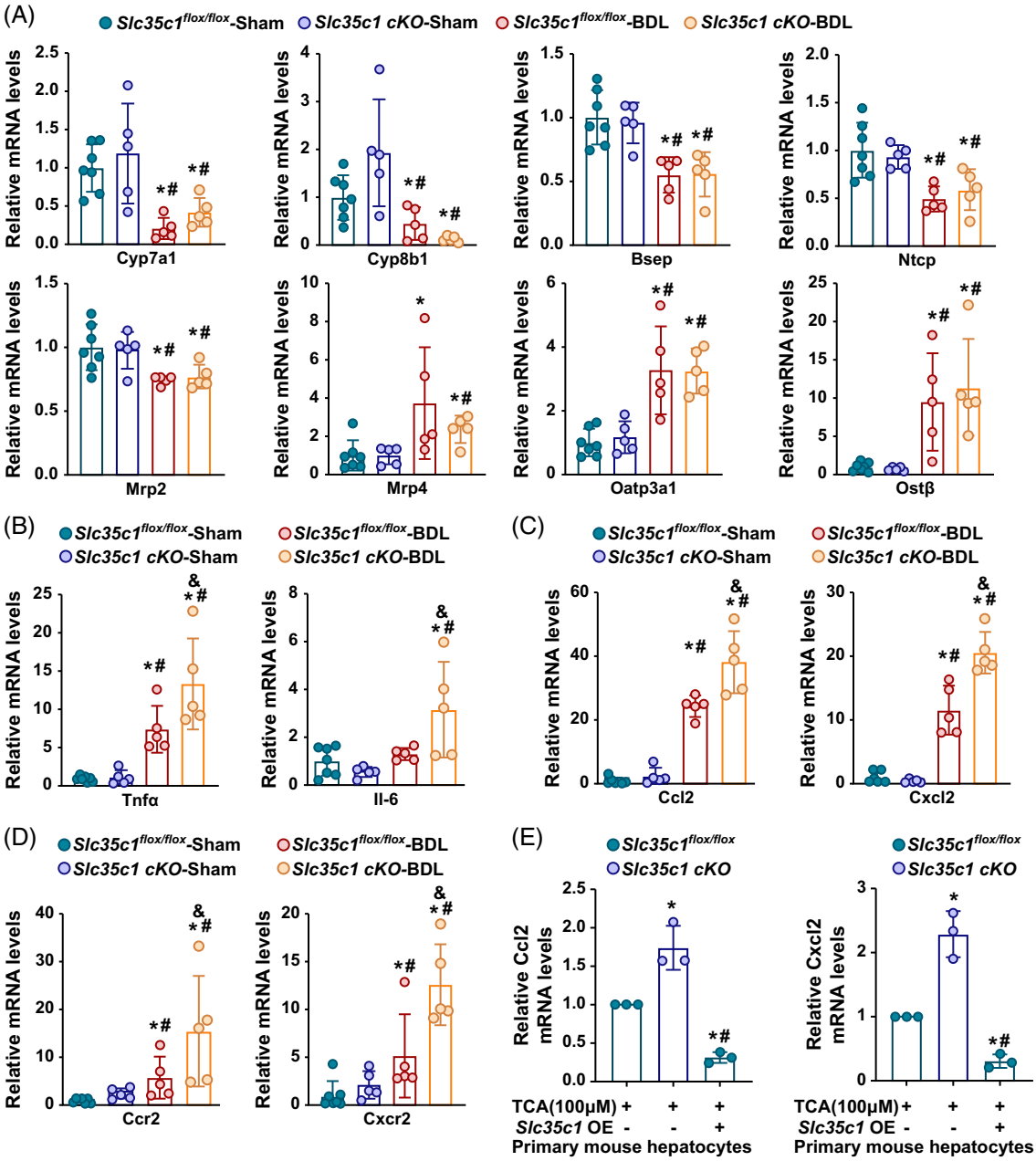

FIGURE 3 Liver-specific *Slc35c1* deficiency aggravates inflammation but does not alter bile acid metabolism in mouse liver. (A) The levels of hepatic mRNA transcripts for the rate-limiting enzymes of bile acid synthesis (Cyp7a1 and Cyp8b1) and the key bile acid transporters (Bsep, Ntcp, Mrp2, Mrp4, Oatp3a1, and Ostβ). (B) The relative levels of hepatic mRNA transcripts for proinflammatory cytokines, Tnfα and Il-6. (C) The relative levels of hepatic Ccl2 and Cxcl2 mRNA transcripts. (D) The relative levels of hepatic Ccr2 and Cxcr2 mRNA transcripts. $^{*}p < 0.05$ vs. the *Slc35c1*$^{flox/flox}$-sham mice; $^{\#}p < 0.05$ vs. the *Slc35c1 cKO*-sham mice; $^{\&}p < 0.05$ vs. the *Slc35c1*$^{flox/flox}$-BDL mice. (E) The relative levels of Ccl2 and Cxcl2 mRNA transcripts in *Slc35c1*$^{flox/flox}$ and/or *Slc35c1 cKO* primary hepatocytes with, or without, *Slc35c1* overexpression, following treatment with 100 μM TCA. $^{*}p < 0.05$ vs. *Slc35c1*$^{flox/flox}$ hepatocytes with 100 μM TCA; $^{\#}p < 0.05$ versus the *Slc35c1 cKO* hepatocytes with 100 μM TCA. Abbreviations: BDL, bile duct ligation; OE, over-expression; SLC35C1, Solute Carrier Family 35 Member C1; TCA, taurocholic acid.

expression and the EGR1 functions to induce CCL2 and CXCL2 expression in hepatocytes.[32,35,36] It is notable that overexpression of WT CEACAM1 significantly abolished the TCA-upregulated *EGR1* mRNA expression in PLC/PRF/5-*ASBT* cells. In contrast, CEACAM1-N153A mutant overexpression or treatment with 2FF failed to inhibit the TCA-induced expression and activation of EGR1 in these cells (Figure 4D, E and Supplemental Figure S10B, http://links.lww.com/HEP/I541). Interestingly, the CEACAM1-N153A mutant overexpression or treatment with 2FF significantly reduced the fucosylation of CEACAM1 in PLC/PRF/5-*ASBT* cells (Figure 4F, G). Furthermore, pull-down assays revealed that induction of both SLC35C1 and CEACAM1 overexpression dramatically increased the CEACAM1 fucosylation in PLC/PRF/5-

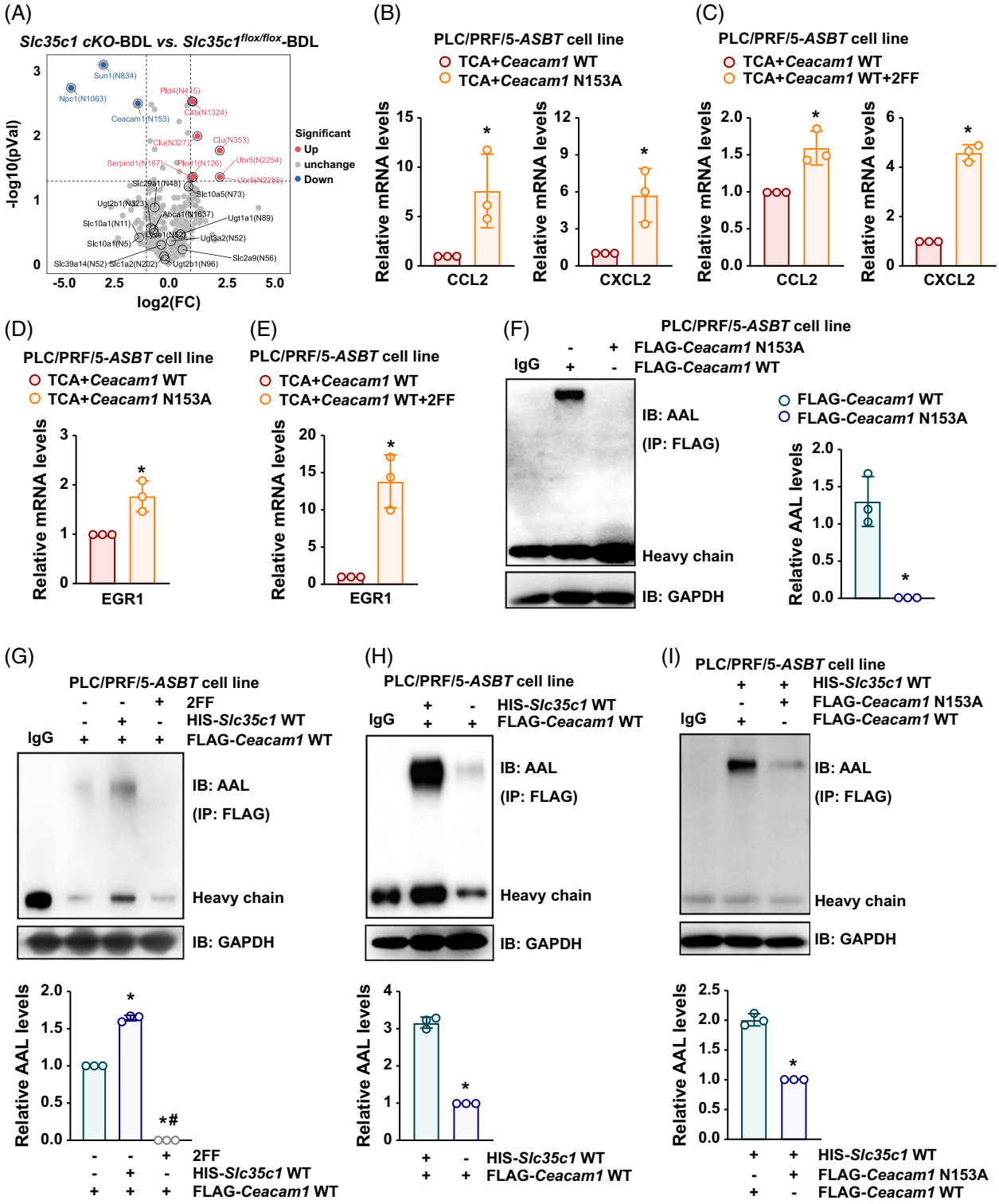

FIGURE 4 Defucosylated CEACAM1 enhances chemokine expressions, whereas SLC35C1 induces the fucosylation of CEACAM1. (A) Volcano plot displayed the quantified N-glycosylated proteins from *Slc35c1*$^{flox/flox}$ and *Slc35c1 cKO*-BDL mouse livers (n = 5 for each group). (B) Induction of *Ceacam1*-WT, but not *Ceacam1*-N153A mutant, overexpression significantly mitigated the 100 μM TCA-upregulated CCL2 and CXCL2 mRNA transcripts in PLC/PRF/5-*ASBT* cells. (C) Treatment with 2FF rescued the 100 μM TCA-upregulated CCL2 and CXCL2 mRNA transcripts in the *Ceacam1*-WT overexpressing PLC/PRF/5-*ASBT* cells. (D) Induction of *Ceacam1*-WT, but not *Ceacam1*-N153A mutant, overexpression significantly mitigated the 100 μM TCA-upregulated EGR1 mRNA transcripts in PLC/PRF/5-*ASBT* cells. (E) Treatment with 2FF rescued the 100 μM TCA-upregulated EGR1 mRNA transcripts in the *Ceacam1*-WT overexpressing PLC/PRF/5-*ASBT* cells. *$p < 0.05$ vs. the cells that had been transfected with *Ceacam1*-WT plasmid and treated with TCA, which was designated as 1 (n = 3). (F) The levels of fucosylated Ceacam1 in PLC/PRF/5-*ASBT* cells transfected with *Ceacam1*-WT or *Ceacam1*-N153A plasmid. *$p < 0.05$ vs. the cells transfected with *Ceacam1*-WT plasmid (n = 3). (G) The levels of fucosylated CEACAM1 in PLC/PRF/5-*ASBT* cells that had been co-transfected with the plasmids for

SLC35C1-WT and *Ceacam1*-WT overexpression or treated with 2FF. *$p < 0.05$ vs. the cells transfected with *Ceacam1*-WT plasmid. #$p < 0.05$ vs. the cells co-transfected with *Ceacam1*-WT and *Slc35c1*-WT (n = 3). (H) The levels of fucosylated Ceacam1 in PLC/PRF/5-*ASBT* cells that had been transfected with *Ceacam1*-WT plasmid or co-transfected with *Ceacam1*-WT and *Slc35c1*-WT plasmids. *$p < 0.05$ vs. the cells that had been co-transfected with *Ceacam1*-WT and *Slc35c1*-WT plasmids (n = 3). (I) The levels of fucosylated Ceacam1 in PLC/PRF/5-*ASBT* cells that had been co-transfected with *Slc35c1*-WT and *Ceacam1*-WT plasmids or *Ceacam1*-N153A mutant plasmid. *$p < 0.05$ vs. the cells co-transfected with *Ceacam1*-WT and *Slc35c1*-WT (n = 3). Abbreviations: AAL, aleuria aurantia lectin; *ASBT*, apical sodium-dependent; BA transporter; BDL, bile duct ligation; HIS, histidine; IB, immunoblots; IP, immunoprecipitation; 2FF, 2-fluorofucose; PLC, primary liver carcinoma; PRF, Poliomyelitis Research Foundation; TCA, taurocholic acid; WT, wild type.

ASBT cells (Figure 4H). In contrast, overexpression of SLC35C1 did not enhance the fucosylation of exogenously expressed CEACAM1-N153A mutant in PLC/PRF/5-*ASBT* cells (Figure 4I). To further examine whether SLC35C2 can facilitate the fucosylation of CEACAM1, we constructed the plasmids for the expression of Ceacam1-WT and Slc35c2, and transfected them into PLC/PRF/5-*ASBT* cells. Pull-down assays revealed that SLC35C2 overexpression did not enhance the CEACAM1 fucosylation in PLC/PRF/5-*ASBT* cells (Supplemental Figure S1E, http://links.lww.com/HEP/I541). Together, these data indicated that SLC35C1 promoted the fucosylation of CEACAM1 at N153, which may repress the BA-upregulated CCL2 and CXCL2 expression through EGR1 in hepatocytes.

Conjugated BAs significantly stimulate the expression of SLC35C1 in primary mouse hepatocytes and PLC/PRF/5-ASBT cells

To further reveal the regulatory mechanism of SLC35C1 expression during the process of cholestasis, we tested whether conjugated BAs could stimulate SLC35C1 expression in hepatocytes. As shown in Figure 5A, B, treatment with conjugated BAs, including TCA, taurochenodeoxycholic acid, glycocholic acid, glycochenodeoxycholic acid, and taurodeoxycholic acid, significantly increased Slc35c1 mRNA and protein expression in primary mouse hepatocytes. Similar results were obtained in human PLC/PRF/5-*ASBT* cells (Figure 5C, D). Furthermore, real-time quantitative PCR and western blotting analyses showed that TCA treatment induced SLC35C1 mRNA and protein expression in a dose-dependent manner in human PLC/PRF/5-*ASBT* cells (Figure 5E, F). These data demonstrated that conjugated BAs effectively stimulated SLC35C1 expression in hepatocytes.

Transcriptional factor STAT3 binding to the SLC35C1 promoter directly induces SLC35C1 expression in cholestatic hepatocytes and mouse livers

To investigate how conjugated BAs stimulated SLC35C1 expression in cholestatic hepatocytes, we performed *in silico* analysis of human *SLC35C1* promoter region and identified 4 putative STAT3 response elements using JASPAR (http://jaspar.genereg.net) (Figure 6A). To explore whether activated STAT3 could regulate SLC35C1 expression, PLC/PRF/5-*ASBT* cells were stimulated with conjugated BAs in the presence or absence of APTSTAT3-9R, a STAT3 inhibitor. As shown in Figure 6B, TCA treatment increased STAT3 phosphorylation, indicating its activation, and treatment with APTSTAT3-9R, an inhibitor of STAT3 diminished the BA-enhanced SLC35C1 protein expression. These observations indicated that activated STAT3 stimulated SLC35C1 expression in cholestatic hepatocytes. Our studies and those of others have shown that ER stress can activate STAT3,[37,38] and BAs cause ER stress in mouse hepatocytes.[5] Next, we explored whether BAs could induce ER stress in human hepatoma cells. We found that treatment with 100 μM TCA led GRP78 leaking from the ER to the cytosol in PLC/PRF/5-*ASBT* cells (Figure 6C). Together, these findings indicate that BAs stimulated ER stress and activation of STAT3, which associated with the upregulation of SLC35C1 in PLC/PRF/5-*ASBT* cells.

To validate whether the putative STAT3 response elements are functional, 4 reporter constructs were generated and contained different regions of the *SLC35C1* promoter (−1806, −898, −342, −272 to +36, respectively). Dual-luciferase reporter analysis indicated that the response element located at −898 to −342 was crucial for the TCA-induced *SLC35C1* promoter activity in PLC/PRF/5-*ASBT* cells (Figure 6D). Co-transfection of a STAT3 expression construct significantly increased the *SLC35C1* promoter-controlled luciferase activity in PLC/PRF/5-*ASBT* cells, which was further enhanced by treatment with TCA (Figure 6E). However, these inductions were abolished when the putative STAT3 response element in the *SLC35C1* promoter (pGL3: −898/+36) was mutated (Figure 6F). ChIP assays exhibited that TCA enhanced the binding of STAT3 to the *SLC35C1* promoter (region: −827 to −817), which was abrogated by treatment with APTSTAT3-9R in PLC/PRF/5-*ASBT* cells (Figure 6G). Similar results were observed in liver samples of patients with OC and cholestatic mouse models. As shown in Figure 6H–J, the binding of hepatic STAT3 to the *SLC35C1* promoter (human region: −827 to −817; mouse region: −693 to −684) was significantly higher in patients with OC, BDL mice, and 1% CA-fed mice, when compared with their corresponding controls. Altogether, these data demonstrated that conjugated BAs activated the STAT3 signaling and stimulated SLC35C1 expression in cholestatic livers.

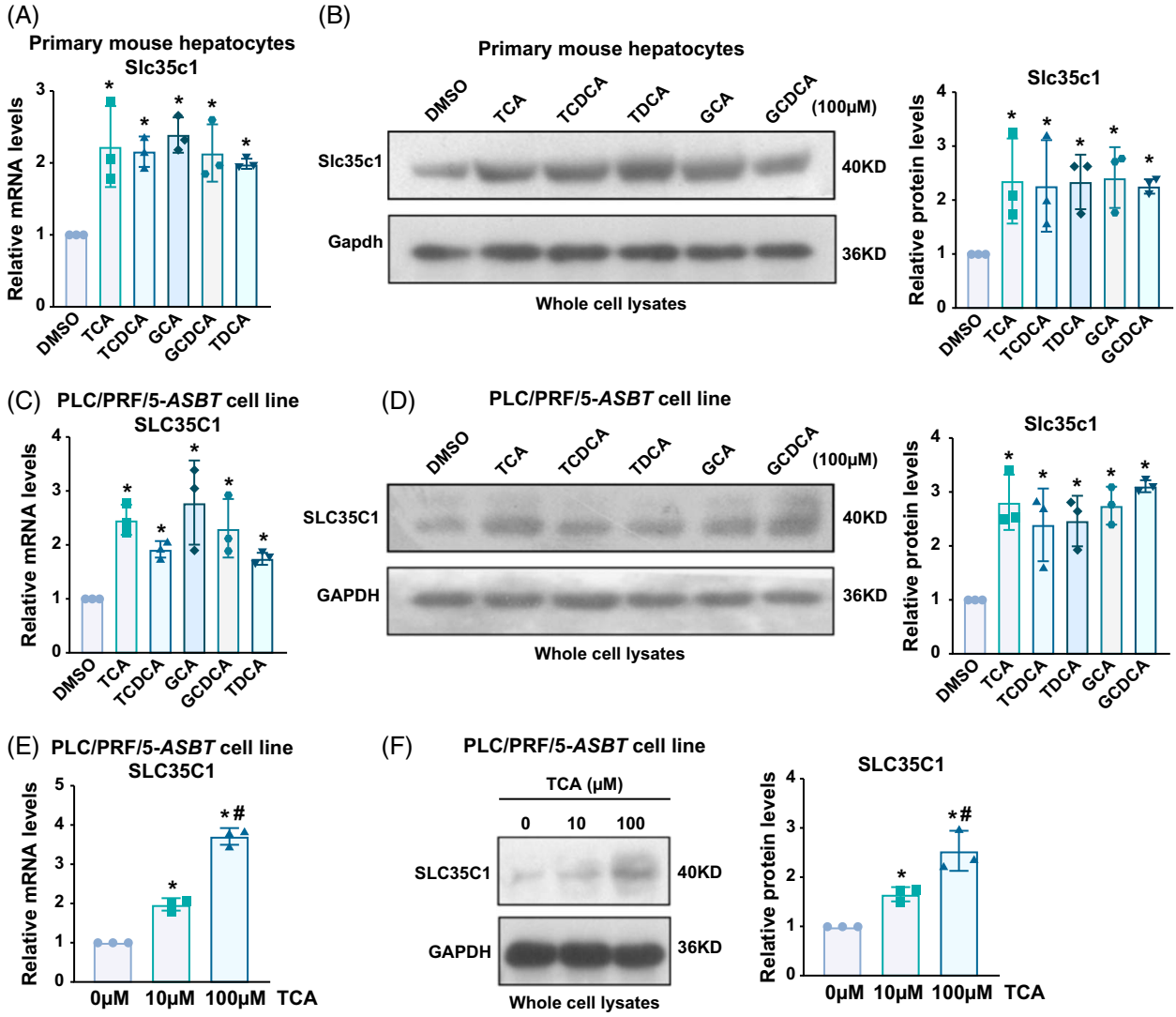

FIGURE 5 Conjugated BAs stimulate SLC35C1 expression in human and mouse hepatocytes. (A, B) The relative levels of Slc35c1 mRNA transcripts and protein expression in primary mouse hepatocytes treated with conjugate bile acids (including 100 μM TCA, TCDCA, GCA, GCDCA, and taurodeoxycholate acid/TDCA). (C, D) The relative levels of SLC35C1 mRNA transcripts and protein expression in PLC/PRF/5-*ASBT* cells following treatment with one type of conjugate bile acids above. $^{*}p < 0.05$ vs. the control (DMSO) group (n = 3). (E, F) The relative levels of SLC35C1 mRNA transcripts and protein expression in PLC/PRF/5-*ASBT* cells following treatment with different doses of TCA. $^{*}p < 0.05$ vs. the DMSO group; $^{\#}p < 0.05$ vs. the cells treated with 10 μM TCA group (n = 3). Abbreviations: GAPDH, glyceraldehyde-3-phosphate dehydrogenase; GCA, glycocholic acid; GCDCA, glycochenodexycholic acid; PLC, primary liver carcinoma; PRF, Poliomyelitis Research Foundation; SLC35C1, Solute Carrier Family 35 Member C1; TCA, taurocholic acid; TCDCA, taurochenodeoxycholic acid TDCA, taurodeoxycholic acid.

DISCUSSION

In this study, we studied the functional role of SLC35C1 and the regulation of its expression in the liver with cholestasis. We found that (1) SLC35C1 expression was upregulated in hepatocytes from both cholestatic and murine models of cholestasis (Figure 1 and Supplemental Figure S2, http://links.lww.com/HEP/I541); (2) liver-specific ablation of *Slc35c1* aggravated liver injury in mouse cholestatic models by increasing hepatic inflammation and reducing Ceacam1 N153 fucosylation (Supplemental Tables S7, S8, http://links.lww.com/HEP/I541, Figure 2, Figure 3B–D and Figure 4A); (3) *Slc35c1* deficiency enhanced the BA-stimulated Ccl2 and Cxcl2 expression in primary mouse hepatocytes (Figure 3E); (4) SLC35C1 (but not SLC35C2) overexpression increased CEACAM1 glycosylation and decreased the BA-stimulated EGR1, CCL2, and CXCL2 expression in PLC/PRF/5-*ASBT* cells; these outcomes were reversed by CEACAM1 N153A mutation or inhibition of fucosylation (Figure 4B–I, Supplemental Figures S1, S10, http://links.lww.com/HEP/I541); (5) gene reporter assay revealed a STAT3 response element in the human *SLC35C1* promoter (Figure 6). (6) blocking STAT3 activation diminished the BA-stimulated *SLC35C1* promoter-controlled luciferase activity and endogenous SLC35C1 mRNA expression (Figures 5, 6). Therefore, upregulated SLC35C1

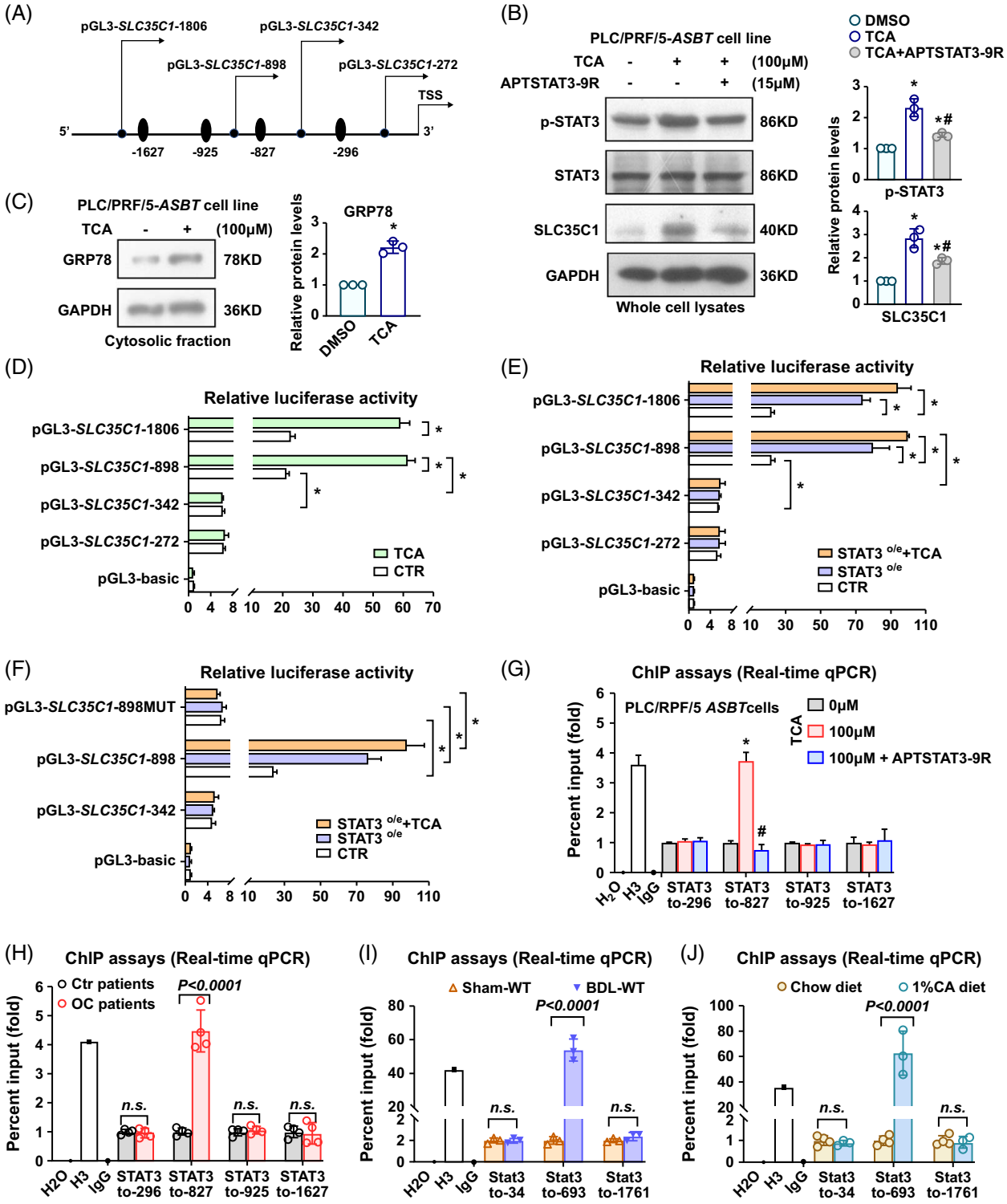

FIGURE 6 Conjugated bile acids enhance the binding of activated STAT3 to the *SLC35C1* promoter to directly induce SLC35C1 expression in cholestasis. (A) A diagram illustrated the potential STAT3 binding sites in human *SLC35C1* proximal promoter and the reporter constructs. (B) Treatment with TCA-induced STAT3 activation and SLC35C1 expression in PLC/PRF/5-*ASBT* cells, which was mitigated by treatment with a STAT3-specific inhibitor (APTSTAT3-9R). n = 3, $^{*}p < 0.05$ vs. the DMSO group; $^{\#}p < 0.05$ vs. the cells treated with 100 μM TCA alone. (C) Representative western blot detecting leakage of endoplasmic reticulum protein Grp78 into the cytosol in mouse hepatocytes after a 24-hour treatment with 100 μM TCA. n = 3, $^{*}p < 0.05$ vs. the DMSO group. (D) PLC/PRF/5-*ASBT* cells were transiently transfected with 4 different truncated *SLC35C1* promoters and treated with or without TCA. Their luciferase activities were measured. (E) PLC/PRF/5-*ASBT* cells were co-transfected with 4 different truncated *SLC35C1* promoters and the plasmid for *STAT3* overexpression or control, with or without TCA treatment. (F) PLC/PRF/5-*ASBT* cells were co-transfected with WT or mutant *SLC35C1* promoter region and the plasmid for *STAT3* overexpression or control, with or without TCA treatment. $^{*}p < 0.05$. (G) ChIP assays revealed that the TCA-induced STAT3 binding to the *SLC35C1*-827 was abrogated by

treatment with APTSTAT3-9R in PLC/PRF/5-*ASBT* cells. *$p < 0.05$ vs. the cells treated without TCA; #$p < 0.05$ vs the cells treated with 100 μM TCA. (H) ChIP assays displayed the binding of activated STAT3 to the *SLC35C1*-827 in liver tissues of patient with OC. (I, J) ChIP assays exhibited the binding of activated Stat3 to the *Slc35c1*-693 in the livers of BDL mouse model and 1% CA-fed mouse model. Abbreviations: BDL, bile duct ligation; ChIP, chromatin immunoprecipitation; CTR, control; GAPDH, glyceraldehyde-3-phosphate dehydrogenase; PLC, primary liver carcinoma; PRF, Poliomyelitis Research Foundation; SLC35C1, Solute Carrier Family 35 Member C1; RPF, Poliomyelitis Research Foundation; TCA, taurocholic acid; qPCR, quantitative polymerase chain reaction; WT, wild type.

expression in cholestasis represents a novel mechanism to protect liver from cholestatic injury by fucosylating CEACAM1 to repress BA-induced CCL2 and CXCL2 expression and inflammation (Figure 7).

Studies have revealed that a mutation in SLC35C1 results in LADII due to deficiency of leukocyte adhesion, but the mechanism remains unclear.[14] In this study, we found that loss of *Slc35c1* significantly reduced the N-glycosylation levels of Ceacam1, Npc1, and Sun1 in the livers of *Slc35c1*-deficient mice following BDL-induced cholestasis, suggesting that Slc35c1 may directly facilitate the N-glycosylation of these proteins in the liver. Among these 3 proteins, CEACAM1 is the only cell surface membrane protein involved in cell adhesion.[25] Therefore, we propose that the deficiency of leukocyte adhesion in patients with LADII may be due to the compromised function of CEACAM1 in these patients. Because CEACAM1 acts as a cell surface co-inhibitory receptor and is expressed on a variety of immune and parenchymal cells, CEACAM1 can modulate immune responses and repress inflammation by inhibiting natural killer cell-mediated cytotoxicity and neutrophil and macrophage functions.[39,40] CEACAM1 can also regulate T-cell activation and repress inflammation during the process of inflammatory bowel disease and chronic viral infection.[41,42] We found that hepatic *Slc35c1* deficiency decreased the fucosylation of Ceacam1 at N153, which was associated with stronger inflammation (evidenced by increased infiltrates of neutrophils, macrophages, T cells, and elevated expression of inflammatory genes) in the livers of mice following BDL-induced cholestasis (Figures 2–4 and Supplemental Figure S5, http://links.lww.com/HEP/I541); also the lack of CEACAM1 N153 glycosylation or inhibition of Ceacam1 fucosylation by 2FF significantly increased the BA-stimulated EGR1, CCL2, and CXCL2 expression in PLC/PRF/5-*ASBT* cells. Therefore, we conclude that the enhanced cholestatic liver injury in *Slc35c1*-deficient mice is most likely due to the lack of Ceacam1 N153 fucosylation, leading to stronger inflammation in the mice. This conclusion agrees with other reports,[25,26] supporting the notion that CEACAM1 protects tissues from inflammatory injury. Although CEACAM1 mRNA and protein expression were

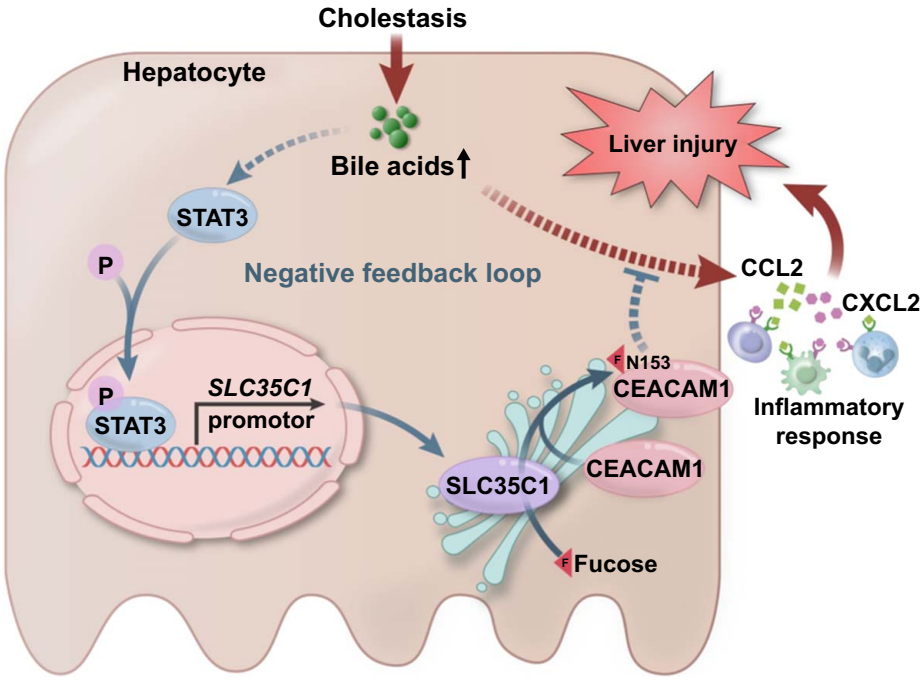

FIGURE 7 A schematic diagram illustrates a novel negative feedback loop against cholestatic liver injury and inflammation. Initially, the accumulated BAs in the liver trigger inflammatory responses and cause liver injury during the process of cholestasis.[5] Meanwhile, BAs also activate the STAT3 signaling and enhance the binding of activated STAT3 to the *SLC35C1* promoter to upregulate SLC35C1 expression in hepatocytes. Finally, elevated SLC35C1 expression facilitates CEACAM1 fucosylation, which in turn suppresses CCL2 and CXCL2 expression to inhibit liver inflammation during the process of cholestasis. Abbreviation: SLC35C1, Solute Carrier Family 35 Member C1.

decreased in cholestatic livers from both patients and mouse models (Supplemental Figure S9B, E, http://links.lww.com/HEP/I541), its fucosylation was significantly increased (Supplemental Figure S9F, http://links.lww.com/HEP/I541), suggesting that there are multiple mechanisms involved in regulating CEACAM1 function, one by transcription, another by post-translation modification (eg, glycosylation). Since overexpression of Ceacam1 in mice protects the liver from high-fat–induced injury,[24] and we also found that CEACAM1 overexpression significantly abolished the TCA-induced *CCL2* and *CXCL2* mRNA expression in PLC/PRF/5-*ASBT* cells (Supplemental Figure S10A, http://links.lww.com/HEP/I541), we propose that CEACAM1 mediates inflammatory response in cholestasis, and its N153 fucosylation reduces liver inflammation and injury. Since CEACAM1 has multiple glycosylation sites, it is possible that the functional significances of these glycosylation sites and or the composition of the saccharide moieties are different. Specifically, we hypothesize that fucosylation of N153 in CEACAM1 may try to stabilize CEACAM1 or affect its homophilic and/or heterophilic binding and mitigate inflammatory response. However, because Slc35c1 deficiency also decreased the fucosylation of Npc1 and Sun1 in the cholestatic livers, and these genes are also potentially involved in immune responses and inflammation,[43,44] we cannot exclude a similar role of these proteins in regulating the process of cholestatic liver injury in these animal models. It would be interesting to know whether the fucosylation and function of CEACAM1, NPC1, and SUN1 are altered in patients with LADII. Future studies may address these questions.

Upregulated SLC35C1 expression has been observed in liver cancers, such as HCC and iCCA, but the functional role of SLC35C1 and what causes their upregulated expression remain unknown. In this study, we found that hepatic SLC35C1 (but not SLC35C2) expression was significantly upregulated in patients with cholestasis and mouse models of cholestasis (Figure 1 and Supplemental Figures S1, S2, http://links.lww.com/HEP/I541). Further in vitro studies indicated that treatment with BA significantly upregulated SLC35C1 (but not SLC35C2 or CEACAM1) expression in both primary mouse hepatocytes and human PLC/PRF/5-*ASBT* cells (Figure 5, Supplemental Figure S1B, http://links.lww.com/HEP/I541 and Supplemental Figure S9A, http://links.lww.com/HEP/I541). Luciferase reporter assay revealed that BA-activated STAT3 during cholestasis was responsible for the upregulation of SLC35C1 expression in hepatocytes by binding to its response element at −898 to −342 in the *SLC35C1* promoter (Figure 6). The role of STAT3 in regulating SLC35C1 expression in cholestasis was further confirmed in vitro in PLC/PRF/5-*ASBT* cells as blocking STAT3 activation reduced the BA-stimulated SLC35C1 expression (Figure 6B), and in vivo in liver tissues from patients with OC and BDL mice using ChIP assay (Figure 6H–J). However, how BAs trigger STAT3 activation remains to be elucidated, although we found that this activation is associated with BA-induced ER stress[5] (Figure 6C). Studies also indicate that ER stress activates STAT3.[37,38] Our study has also shown that hepatic STAT3 signaling is activated in patients with cholestasis, reducing chemokine expression.[7] Therefore, it is reasonable to believe that the upregulated SLC35C1 expression in cholestatic liver stemmed from the activation of STAT3 signaling in hepatocytes. This may also explain why increased SLC35C1 expression is detected in HCC and iCCA as activated STAT3 signaling has been found in these diseases.[15,16] Therefore, we also speculate that the upregulated SLC35C1 expression in HCC and iCCA may modulate immune and inflammatory responses during their progression. Finally, we found that SLC35C1 expression was upregulated in the livers of patients with cholestasis and all 4 cholestatic mouse models (BDL mice, 1% CA-fed mice, 0.1% DDC-fed mice, as well as *Abcb4*-KO mice), suggesting that this upregulation is likely an adaptive response to reduce cholestatic liver injury. However, because the severities of liver injury in these animal models are different, it is possible that the functional significance of Slc35c1 in these models may be varying.

In conclusion, our data indicate that upregulated hepatic SLC35C1 expression protects the liver from cholestatic injury by enhancing CEACAM1 fucosylation to suppress the BA-stimulated chemokine CCL2 and CXCL2 expression and inflammation. The upregulated SLC35C1 expression is mediated through the activation of hepatic STAT3 signaling during the process of cholestasis. These findings suggest that stimulation of hepatic SLC35C1 expression might be a novel strategy to treat cholestasis.

AUTHOR CONTRIBUTIONS

Jin Chai conceived the study; Jin Chai, Qiong Pan, Shi-Ying Cai, and Wensheng Chen designed the study; Liangjun Zhang, Pingfan Xie, Mingqiao Li, Qiong Pan, Xiaoxun Zhang, Shuke Fei, Nan Zhao, Qiaoling Xie, Ziqian Xu, and Wan Tang performed the experiments; Liangjun Zhang, Pingfan Xie, Mingqiao Li, Qiong Pan, and Ling Li collected the data; Liangjun Zhang, Shuke Fei, Pingfan Xie, Mingqiao Li, and Qiong Pan performed the statistical analysis; Zhixian Zhu, Zuzhi Xu, Guanyu Zhu, Jianwei Li, and Chengcheng Zhang contributed to special reagents/analysis tools; Jin Chai, Pingfan Xie, Qiong Pan, Shi-Ying Cai, and James L. Boyer wrote the manuscript.

ACKNOWLEDGMENTS

The authors thank Dr Ruilin Sun (Shanghai Model Organisms Center Inc., Shanghai, China) and our team members (Cholestatic Liver Diseases Center and Center for Metabolic Associated Fatty Liver Disease, Southwest Hospital, Third Military Medical University, Chongqing, China) for the technical assistance.

FUNDING INFORMATION

This work is supported by grants from the National Natural Science Foundation of China (82325008, 92268110, and 82370561), the Outstanding Youth Foundation of Chongqing (cstc2021jcyj-jqX0005), the Project of Chongqing Universities Innovation Research/Outstanding Medical Research Group (2021cqspt01 and 414Z381).

CONFLICTS OF INTEREST

The authors have no conflicts to report.

ORCID

Liangjun Zhang https://orcid.org/0000–0002–7053–8661
Pingfan Xie https://orcid.org/0009–0008–9443–8340
Mingqiao Li https://orcid.org/0000–0003–3692–2552
Xiaoxun Zhang https://orcid.org/0000–0002–1342–2507
Shuke Fei https://orcid.org/0000–0002–3354–2274
Nan Zhao https://orcid.org/0000–0002–4597–6547
Ling Li https://orcid.org/0000–0002–9027–7307
Qiaoling Xie https://orcid.org/0000–0002–1342–2507
Ziqian Xu https://orcid.org/0009–0005–2809–5130
Wan Tang https://orcid.org/0000–0001–5693–3342
Guanyu Zhu https://orcid.org/0009–0003–1601–5928
Zhixian Zhu https://orcid.org/0009–0002–9654–6421
Zuzhi Xu https://orcid.org/0009–0006–0852–0432
Jianwei Li https://orcid.org/0000–0001–9629–7475
Chengcheng Zhang https://orcid.org/0000–0002–0550–107X
James L. Boyer https://orcid.org/0000–0002–8959–6036
Shi-Ying Cai https://orcid.org/0000–0001–6601–4040
Qiong Pan https://orcid.org/0000–0003–1033–3098
Jin Chai https://orcid.org/0000–0002–8543–4566

REFERENCES

1. Poupon R, Chazouillères O, Poupon RE. Chronic cholestatic diseases. J Hepatol. 2000;32:129–40.
2. Wagner M, Fickert P. Drug therapies for chronic cholestatic liver diseases. Annu Rev Pharmacol Toxicol. 2020;60:503–27.
3. Zhang Y, Hong JY, Rockwell CE, Copple BL, Jaeschke H, Klaassen CD. Effect of bile duct ligation on bile acid composition in mouse serum and liver. Liver Int. 2012;32:58–69.
4. Sasaki M, Miyakoshi M, Sato Y, Nakanuma Y. Chemokine-chemokine receptor CCL2-CCR2 and CX3CL1-CX3CR1 axis may play a role in the aggravated inflammation in primary biliary cirrhosis. Dig Dis Sci. 2014;59:358–64.
5. Cai SY, Ouyang X, Chen Y, Soroka CJ, Wang J, Mennone A, et al. Bile acids initiate cholestatic liver injury by triggering a hepatocyte-specific inflammatory response. JCI Insight. 2017;2:e90780.
6. Zhang X, Li L, Zhao N, Pan Q, Zhang L, Xie Q, et al. A novel role for interleukin 32 in cholestasis. Clin Transl Med. 2021;11:e594.
7. Zhang L, Pan Q, Zhang L, Xia H, Liao J, Zhang X, et al. Runt-related transcription factor-1 ameliorates bile acid-induced hepatic inflammation in cholestasis through JAK/STAT3 signaling. Hepatology. 2023;77:1866–81.
8. Lu L, Hou X, Shi S, Körner C, Stanley P. Slc35c2 promotes Notch1 fucosylation and is required for optimal Notch signaling in mammalian cells. J Biol Chem. 2010;285:36245–54.
9. Zhang P, Haryadi R, Chan KF, Teo G, Goh J, Pereira NA, et al. Identification of functional elements of the GDP-fucose transporter SLC35C1 using a novel Chinese hamster ovary mutant. Glycobiology. 2012;22:897–911.
10. Song Z. Roles of the nucleotide sugar transporters (SLC35 family) in health and disease. Mol Aspects Med. 2013;34:590–600.
11. Sturla L, Rampal R, Haltiwanger RS, Fruscione F, Etzioni A, Tonetti M. Differential terminal fucosylation of N-linked glycans versus protein O-fucosylation in leukocyte adhesion deficiency type II (CDG IIc). J Biol Chem. 2003;278:26727–33.
12. Etzioni A, Frydman M, Pollack S, Avidor I, Phillips ML, Paulson JC, et al. Brief report: recurrent severe infections caused by a novel leukocyte adhesion deficiency. N Engl J Med. 1992;327:1789–92.
13. Lübke T, Marquardt T, Etzioni A, Hartmann E, von Figura K, Körner C. Complementation cloning identifies CDG-IIc, a new type of congenital disorders of glycosylation, as a GDP-fucose transporter deficiency. Nat Genet. 2001;28:73–6.
14. Lühn K, Wild MK, Eckhardt M, Gerardy-Schahn R, Vestweber D. The gene defective in leukocyte adhesion deficiency II encodes a putative GDP-fucose transporter. Nat Genet. 2001;28:69–72.
15. Moriwaki K, Noda K, Nakagawa T, Asahi M, Yoshihara H, Taniguchi N, et al. A high expression of GDP-fucose transporter in hepatocellular carcinoma is a key factor for increases in fucosylation. Glycobiology. 2007;17:1311–20.
16. Ament CE, Steinmann S, Evert K, Pes GM, Ribback S, Gigante I, et al. Aberrant fucosylation sustains the NOTCH and EGFR/NF-kappaB pathways and has a prognostic value in human intrahepatic cholangiocarcinoma. Hepatology. 2023;78:1742–54.
17. Kammerer R, Zimmermann W. Coevolution of activating and inhibitory receptors within mammalian carcinoembryonic antigen families. BMC Biol. 2010;8:12.
18. Prall F, Nollau P, Neumaier M, Haubeck HD, Drzeniek Z, Helmchen U, et al. CD66a (BGP), an adhesion molecule of the carcinoembryonic antigen family, is expressed in epithelium, endothelium, and myeloid cells in a wide range of normal human tissues. J Histochem Cytochem. 1996;44:35–41.
19. Cruz PV, Wakai T, Shirai Y, Yokoyama N, Hatakeyama K. Loss of carcinoembryonic antigen-related cell adhesion molecule 1 expression is an adverse prognostic factor in hepatocellular carcinoma. Cancer. 2005;104:354–60.
20. Horst AK, Wegscheid C, Schaefers C, Schiller B, Neumann K, Lunemann S, et al. Carcinoembryonic antigen-related cell adhesion molecule 1 controls IL-2-dependent regulatory T-cell induction in immune-mediated hepatitis in mice. Hepatology. 2018;68:200–14.
21. Kelleher M, Singh R, O'Driscoll CM, Melgar S. Carcinoembryonic antigen (CEACAM) family members and inflammatory bowel disease. Cytokine Growth Factor Rev. 2019;47:21–31.
22. Schirbel A, Rebert N, Sadler T, West G, Rieder F, Wagener C, et al. Mutual regulation of TLR/NLR and CEACAM1 in the intestinal microvasculature: Implications for IBD pathogenesis and therapy. Inflamm Bowel Dis. 2019;25:294–305.
23. Muturi HT, Ghadieh HE, Abdolahipour R, Stankus HL, Belew GD, Liu JK, et al. Loss of CEACAM1 in endothelial cells causes hepatic fibrosis. Metabolism. 2023;144:155562.
24. Al-Share QY, DeAngelis AM, Lester SG, Bowman TA, Ramakrishnan SK, Abdallah SL, et al. Forced hepatic overexpression of CEACAM1 curtails diet-induced insulin resistance. Diabetes. 2015;64:2780–90.
25. Huang YH, Zhu C, Kondo Y, Anderson AC, Gandhi A, Russell A, et al. CEACAM1 regulates TIM-3-mediated tolerance and exhaustion. Nature. 2015;517:386–90.
26. Nakamura K, Kageyama S, Kaldas FM, Hirao H, Ito T, Kadono K, et al. Hepatic CEACAM1 expression indicates donor liver quality

and prevents early transplantation injury. J Clin Invest. 2020;130:2689–704.
27. Lucka L, Sel S, Danker K, Horstkorte R, Reutter W. Carcinoembryonic antigen-related cell-cell adhesion molecule C-CAM is greatly increased in serum and urine of rats with liver diseases. FEBS Lett. 1998;438:37–40.
28. Dráberová L, Černá H, Brodská H, Boubelík M, Watt SM, Stanners CP, et al. Soluble isoforms of CEACAM1 containing the A2 domain: Increased serum levels in patients with obstructive jaundice and differences in 3-fucosyl-N-acetyl-lactosamine moiety. Immunology. 2000;101:279–87.
29. Li X, Li Y, Xiao J, Wang H, Guo Y, Mao X, et al. Unique DUOX2 (+)ACE2(+) small cholangiocytes are pathogenic targets for primary biliary cholangitis. Nat Commun. 2023;14:29.
30. Chen R, Huang B, Lian M, Wei Y, Miao Q, Liang J, et al. A+T rich interaction domain protein 3a (Arid3a) impairs Mertk-mediated efferocytosis in cholestasis. J Hepatol. 2023;79:1478–90.
31. Pan Q, Zhang X, Zhang L, Cheng Y, Zhao N, Li F, et al. Solute carrier organic anion transporter family member 3A1 is a bile acid efflux transporter in cholestasis. Gastroenterology. 2018;155:1578–92 e1516.
32. Pan Q, Zhu G, Xu Z, Zhu J, Ouyang J, Tong Y, et al. Organic anion transporting polypeptide (OATP) 1B3 is a significant transporter for hepatic uptake of conjugated bile acids in humans. Cell Mol Gastroenterol Hepatol. 2023;16:223–42.
33. Huang Y, Zhang HL, Li ZL, Du T, Chen YH, Wang Y, et al. FUT8-mediated aberrant N-glycosylation of B7H3 suppresses the immune response in triple-negative breast cancer. Nat Commun. 2021;12:2672.
34. Pan Q, Xie Y, Zhang Y, Guo X, Wang J, Liu M, et al. EGFR core fucosylation, induced by hepatitis C virus, promotes TRIM40-mediated-RIG-I ubiquitination and suppresses interferon-I antiviral defenses. Nat Commun. 2024;15:652.
35. Kim ND, Moon JO, Slitt AL, Copple BL. Early growth response factor-1 is critical for cholestatic liver injury. Toxicol Sci. 2006;90:586–95.
36. Li J, Zhu X, Zhang M, Zhang Y, Ye S, Leng Y, et al. Limb expression 1-like (LIX1L) protein promotes cholestatic liver injury by regulating bile acid metabolism. J Hepatol. 2021;75:400–13.
37. Di Conza G, Tsai CH, Gallart-Ayala H, Yu YR, Franco F, Zaffalon L, et al. Tumor-induced reshuffling of lipid composition on the endoplasmic reticulum membrane sustains macrophage survival and pro-tumorigenic activity. Nat Immunol. 2021;22:1403–5.
38. Zheng Y, Dai H, Chen R, Zhong Y, Zhou C, Wang Y, et al. Endoplasmic reticulum stress promotes sepsis-induced muscle atrophy via activation of STAT3 and Smad3. J Cell Physiol. 2023;238:582–96.
39. Park DJ, Sung PS, Kim JH, Lee GW, Jang JW, Jung ES, et al. EpCAM-high liver cancer stem cells resist natural killer cell-mediated cytotoxicity by upregulating CEACAM1. J Immunother Cancer. 2020;8:e000301.
40. Hirao H, Kojima H, Dery KJ, Nakamura K, Kadono K, Zhai Y, et al. Neutrophil CEACAM1 determines susceptibility to NETosis by regulating the S1PR2/S1PR3 axis in liver transplantation. J Clin Invest. 2023;133:e162940.
41. Nagaishi T, Chen Z, Chen L, Iijima H, Nakajima A, Blumberg RS. CEACAM1 and the regulation of mucosal inflammation. Mucosal Immunol. 2008;1(Suppl 1):S39–42.
42. Khairnar V, Duhan V, Patil AM, Zhou F, Bhat H, Thoens C, et al. CEACAM1 promotes CD8(+) T cell responses and improves control of a chronic viral infection. Nat Commun. 2018;9:2561.
43. Schwerd T, Pandey S, Yang HT, Bagola K, Jameson E, Jung J, et al. Impaired antibacterial autophagy links granulomatous intestinal inflammation in Niemann-Pick disease type C1 and XIAP deficiency with NOD2 variants in Crohn's disease. Gut. 2017;66:1060–73.
44. Tan CY, Chan PS, Tan H, Tan SW, Lee CJM, Wang JW, et al. Systematic in vivo candidate evaluation uncovers therapeutic targets for LMNA dilated cardiomyopathy and risk of Lamin A toxicity. J Transl Med. 2023;21:690.

How to cite this article: Zhang L, Xie P, Li M, Zhang X, Fei S, Zhao N, et al. Hepatic GDP-fucose transporter SLC35C1 attenuates cholestatic liver injury and inflammation by inducing CEACAM1 N153 fucosylation. Hepatology. 2025;81:774–790. https://doi.org/10.1097/HEP.0000000000001003